

## 8 Particle Physics at DESY/HERA (HERA-B)

P. Robmann and P. Truöl

*in collaboration with:*

the Universities of Heidelberg and Siegen and 31 further institutes from outside Switzerland

(HERA-B)

During the long HERA shutdown period that ended in 2002 many detector components were improved. These include the microstrip gas chamber system of the inner tracker in which we are involved (see also [1] and [2]). Now the experiment performs to full satisfaction and the number of recorded  $J/\psi$  decays, for example, has increased from  $\approx 0.5 \text{ min}^{-1}$  during the year 2000 to  $\approx 20 \text{ min}^{-1}$  in

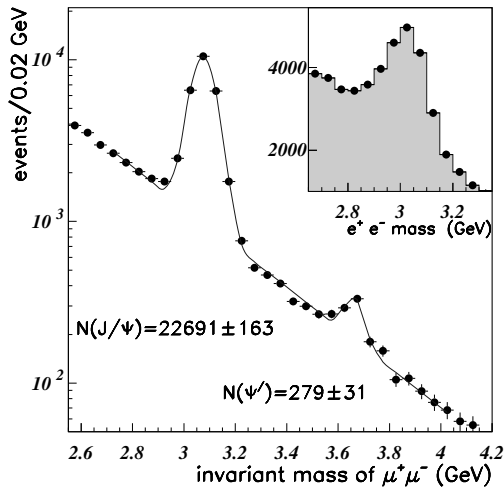


Figure 8.1: Invariant mass spectrum of  $\mu^+\mu^-$  pairs. Charmonium states are clearly seen on an exponentially falling background. The insert shows the corresponding electron distribution.

January 2003. Only a small fraction of these events have been analyzed so far. Figure 8.1 shows the invariant mass distributions of  $\mu^+\mu^-$  and  $e^+e^-$  pairs. Clearly visible are the peaks from  $J/\psi$  and  $\psi'$  decays at  $3.1 \text{ GeV}/c^2$  and  $3.65 \text{ GeV}/c^2$ , respectively.

As a consequence of the better noise performance of the electromagnetic calorimeter, the electron identification no longer has to rely on the existence of bremsstrahlung photons and  $J/\psi$  decays are clearly reconstructible in the channel  $J/\psi \rightarrow e^+e^-$  (Fig. 8.1). Thanks to the increased DAQ bandwidth the event logging rate could be raised from about 40 Hz to more than 1000 Hz. This allowed to take a large sample of minimum bias data in a relatively short time using a simple trigger based on the multiplicities observed in the ring imaging Cerenkov counter (RICH) and the electromagnetic calorimeter (ECAL). These data will

be used both for calibration and for physics analysis of inclusive proton-nucleus collisions.

Different target materials between carbon and tungsten can be used to study  $A$ -dependencies. These measurements give important input for the theoretical understanding of the creation of quark-gluon plasma in heavy-ion collisions and of heavy flavour production in hadronic interactions. To minimize systematic uncertainties several targets of different material can be operated simultaneously. HERA-B is an almost central detector in the proton-nucleon center of mass system. The accessible kinematic region therefore extends to the backward hemisphere with the Feynman's  $x_F < 0$ , which is barely covered by other experiments in this energy regime.

### 8.1 Charmonium production in 920 GeV proton-nucleus interactions

The production mechanism of heavy flavours in hadronic collisions is not well understood and rather different theoretical concepts are used for its description. The Color Singlet Model (CSM) assumes the  $q\bar{q}$  pair to be produced in a color singlet state with the quantum numbers of the final meson. In the

non-relativistic QCD factorization approach (NRQCD) a color singlet or octet quark pair evolves towards the final bound state via exchange of soft gluons while in the Color Evaporation Model (CEM) the exchange of many soft gluons during the formation process of the bound state results in the loss of information about the production mechanism of the  $q\bar{q}$  pair. Charmonium production is an attractive test case as the quarks are heavy enough for perturbative calculations, and the cross sections are large enough to be experimentally accessible. In particular, the dependence of the ratio of production cross sections of different charmonium states like  $R_{\chi_{ci}} = \sigma(\chi_{ci}) / \sigma(J/\psi)$  on center-of-mass energy  $\sqrt{s}$  allows to differentiate between different models. Preferably, the radiative decay  $\chi_{ci} \rightarrow J/\psi\gamma_i$  is measured using the subsequent decay  $J/\psi \rightarrow \ell^+\ell^-$  for triggering. In most experiments the energy resolution is insufficient to resolve the individual  $\chi_{ci}$  states, and one usually quotes the ratio  $R_{\chi_c} = \sum_{i=1}^2 (\sigma(\chi_{ci}) \cdot Br(\chi_{ci} \rightarrow J/\psi)) / \sigma(J/\psi)$  where  $\sigma(J/\psi)$  is the sum of cross sections for direct  $J/\psi$  production and for  $J/\psi$  production from  $\chi_{ci}$  and  $\psi'$  decays. Quite a few experimental data

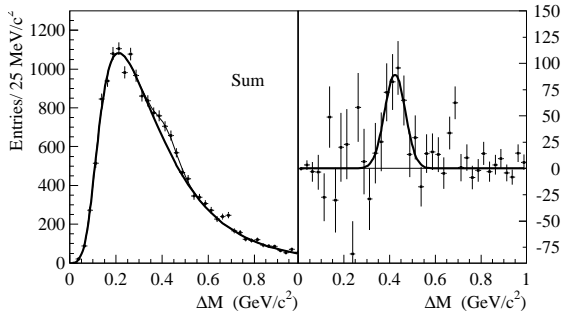


Figure 8.2:  $\Delta M$  distributions (see text). Left: experimental points and combinatorial background from event mixing (solid line). Right:  $\chi_c$  signals after background subtraction.

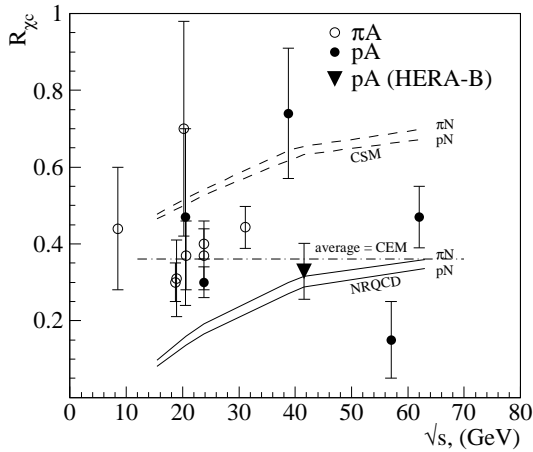


Figure 8.3: Comparison of  $R_{\chi_c}$  values determined in  $pA$  and  $\pi A$  experiments at indicated center-of-mass energies  $\sqrt{s}$ . Error bars include statistical and systematic uncertainties. The dot-dashed line is the average of all measurements. Model predictions based on NRQCD and CSM (see text) are shown by solid and dashed lines, respectively. The CEM predicts a constant value.

are available for values of  $\sqrt{s}$  between 8.5 and 62 GeV but the situation is unclear since experimental errors are in general large. We determined a new value of  $R_{\chi_c}$  at  $\sqrt{s} = 41.6$  GeV [3] based on data collected during a short commissioning run of the  $J/\psi$  trigger in 2000. About half of this data was taken with a single carbon wire target, the rest with carbon and titanium wires together. The detector acceptance for the  $J/\psi$ 's covered a range of  $-0.25 < x_F < 0.15$ .

The  $\chi_c$  is observed in the radiative  $\chi_c$  decay using the difference  $\Delta M$  between the invariant mass of the  $(\ell^+\ell^-\gamma)$  system and the invariant mass of the lepton pair,  $\Delta M = M(\ell^+\ell^-\gamma) - M(\ell^+\ell^-)$ . Fig. 8.2 shows for all combinations of  $J/\psi$  and photon candidates the  $\Delta M$  distribution for the entire data sample. The excess of events above the combinatorial background determines the number of  $\chi_c$  candidates from which  $R_{\chi_c}$  is calculated. Within statistics the results obtained for carbon and titanium are consistent with each other; their average yields a value of  $\langle R_{\chi_c} \rangle = 0.32 \pm 0.06_{stat} \pm 0.04_{sys}$ . Fig. 8.3 compares the HERA-B result with previous data and theoretical predictions; see [3] for a detailed list of references. The HERA-B result is compatible with most of the previous data.

Due to the large errors, a flat energy dependence, as predicted by CEM, cannot be ruled out. Similarly, the slope of the energy dependence as predicted by a Monte Carlo based on NRQCD is also compatible with the data. The absolute value, however, in general seems to be too low, indicating that the NRQCD long distance matrix elements for  $\chi_c$  production are un-

derestimated. On the other hand, CSM predicts  $R_{\chi c}$  to be larger than most of the experimental values. During the 2002 physics run the data sample increased by more than an order of magnitude which will reduce the statistical error of  $R_{\chi c}$  significantly. It will also be possible to study the  $A$ -dependence.

## 8.2 Inclusive $V^0$ production cross sections from 920 GeV fixed target proton-nucleus collisions

One of the main goals of heavy-ion experiments is the observation of the quark-gluon plasma[5] and a possible signature for this state is the enhanced production of strange particles [6]. This led to a renewed interest in strangeness production. Observables of interest are ratios of antibaryons to baryons at mid-rapidity, which are important for net baryon density evaluations and which have been used recently to extract values of chemical potentials and temperatures [7; 8] for Au-Au collisions at RHIC. Also of interest is the transverse momentum distribution which contains information on the temperature of the system after reaching thermal equilibrium (see [9]). These investigations motivate a comprehensive measurement of strange-particle production properties in “ordinary” nucleon-nucleon ( $NN$ ) and nucleon-nucleus ( $NA$ ) collisions. The latter are expected to establish a valuable baseline for comparisons among  $AA$  results [7].

A sample of  $\sim 2.4$  million minimum bias events selected with a random trigger that uniformly sampled all HERA bunches, was taken in 2000 to allow for a precise measurement of strange-particle production cross sections. The inclusive cross sections for  $K_S^0$ ,  $\Lambda$ , and  $\bar{\Lambda}$  particles, collectively referred to as  $V^0$  particles, were determined with various nuclear targets. Experimental details can be found in [4].  $V^0$  candidates were selected from events with track pairs of opposite charge with a vertex downstream of the primary vertex. The primary vertex was required to coincide with the center of a target wire to within three standard deviations. If no primary vertex could be reconstructed, the  $z$ -coordinate of the target was used to calculate the  $z$ -component of the particle’s flight path. The requirement of a minimal flight path reduces the tracks combinatorial background. The invariant mass distributions for the selected candidates are shown in Fig. 8.4. Clear signals corresponding to  $K_S^0$ ,  $\Lambda$ , and  $\bar{\Lambda}$  decays are visible. Based on the Monte-Carlo simulation, the luminosity evaluation and the extrapolation by the Glauber formalism, the production cross section per nucleon was calculated. The result is in good agreement with previous measurements (see Fig. 8.5)

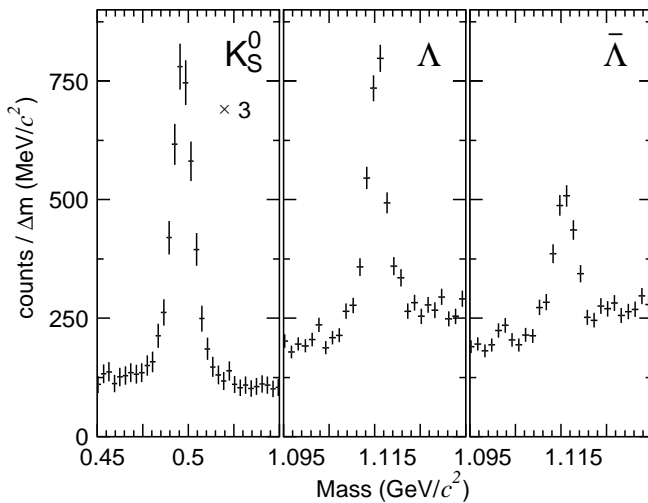


Figure 8.4: Invariant mass distributions for  $K_S^0$ ,  $\Lambda$ , and  $\bar{\Lambda}$  particles summed over all runs with different targets. The bin width  $\Delta m$  is  $3.0 \text{ MeV}/c^2$  for the  $K_S^0$  distribution and  $1.5 \text{ MeV}/c^2$  otherwise.

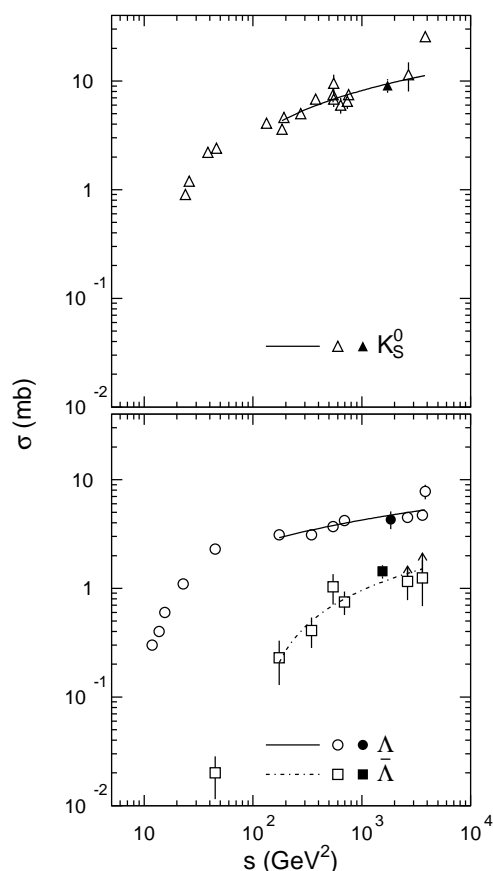


Figure 8.5: The total cross section per nucleon  $\sigma_{pN}$  for the production of  $K_S^0$ ,  $\Lambda$  and  $\bar{\Lambda}$  as a function of the center-of-mass energy squared  $s$ . Full black symbols denote our own results. The curves are fit [12] to the data in the interval 180 - 800 GeV. See [4] for the full references.

- [1] Physik-Institut, Universität Zürich, Annual Report 2001/2, available at <http://www.physik.unizh.ch/jb/2002>.
- [2] *Studies of Aging and HV Breakdown Problems during Development and Operation of MSGC and GEM Detectors for the Inner Tracking System of HERA-B* Y. Bagaturia, O. Baruth, H.B. Dreis, F. Eisele, I. Gorbunov, S. Gradl, W. Gradl, S. Hausmann, M. Hildebrandt, T. Hott, S. Keller, C. Krauss, B. Lomonosov, M. Negodaev, C. Richter, P. Robmann, B. Schmidt, U. Straumann, P. Truöl, S. Visbeck, T. Walter, C. Werner, U. Werthenbach, G. Zech, T. Zehner, and M. Ziegler, hep-ex/0204011, Nucl.Instr.Meth.**A490** (2002), 223 - 242.
- [3] *J/ψ Production via χ<sub>c</sub> Decays in 920 GeV pA Interactions*, The HERA-B Collaboration, I. Abt *et al.*, DESY-02-187, hep-ex/0211033, submitted to Phys.Lett.**B**.
- [4] *Inclusive V<sup>0</sup> Production Cross Sections from 920 GeV Fixed Target Proton-Nucleus Collisions*, The HERA-B Collaboration, I. Abt *et al.*, DESY-02-213, hep-ex/0212040, submitted to Eur.Phys.J.**C**.
- [5] see, e.g., Proc. 15th Int. Conf. on Ultra-Relativistic Nucleus-Nucleus Collisions (QM2001), Nucl.Phys.**A698** (2002) Issue 1-4.
- [6] S. A. Bass *et al.*, Nucl.Phys.**A661** (1999) 205c.
- [7] J. Rafelski *et al.*, nucl-th/0104042.
- [8] P. Braun-Munzinger *et al.* nucl-ph/0105229.
- [9] L. V. Bravina *et al.*, Phys.Rev.**C60** (1999) 024904.
- [10] V. Blobel *et al.*, Nucl.Phys.**B69** (1974) 454.
- [11] M. Asai *et al.*, Z. Phys. **C27** (1985) 11.
- [12] H. Kichimi *et al.*, Phys.Rev.**D20** (1979) 37.